

Electron-phonon interactions in the copper oxides: Implications for the resistivity

Ju H. Kim, K. Levin, and R. Wentzcovitch*

*Department of Physics and the James Franck Institute, The University of Chicago, Chicago, Illinois 60637
and Science and Technology Center for Superconductivity, Chicago, Illinois 60637*

A. Auerbach

Physics Department, Boston University, Boston, Massachusetts 02215

(Received 24 August 1989)

The effects of strong Coulomb correlations on the electron-phonon interaction are calculated using a frozen-phonon approach applied to the extended Hubbard, infinite- U Hamiltonian. As the insulator is approached the electron-phonon interaction becomes progressively weakened due to the inability to transfer charge. Both the magnitude and concentration x dependence of m^*/n are consistent with experiment. While there are no clear experimental trends for variations of $1/\tau$ with x , the magnitude is in agreement with the data. That the calculated electron-phonon contribution to ρ is nearly linear and found to account for most of the observed magnitude must be recognized in estimating the importance of other electronic or magnetic scattering contributions to the linear resistivity.

The temperature-dependent resistivity ρ in the metallic copper oxides is anomalous for a number of reasons: (1) it is linear down to temperatures T low compared to the Debye energy; (2) the slope $d\rho/dT$ is 2 orders of magnitude larger than that of a typical metal such as copper;¹ (3) and there is no indication of saturation effects or even negative values of $d\rho/dT$ such as might have been expected for resistivities in excess of several hundred $\mu\Omega\text{cm}$. Despite these anomalies it is clear, however, that if these materials resemble typical metals in any way, then the electron-phonon scattering contribution to the resistivity should not be ignored. Indeed, it is extremely important to characterize this contribution in order to determine the nature of other scattering mechanisms which may be present.

It is the purpose of the present paper to determine the electron-phonon coupling constants in considerable detail and to thereby deduce the effects of this scattering on the resistivity. While there have been a number of attempts to compute the strength of the electron-phonon coupling^{2,3} and some studies of this contribution to the resistivity,² none of these has taken full account of the role of very strong Coulomb correlations which ultimately drive the system into an insulating state. Furthermore, we believe ours is the first to study systematic carrier concentration effects and to focus on the important constraints provided by the Drude fits to the low-frequency ac conductivity. A Drude analysis makes it possible to decompose the dc conductivity into both a static (but temperature-dependent) scattering time and an m^*/n contribution. A separate measurement of these two quantities provides extremely important information. This determination of the lifetime in $\text{YBa}_2\text{Cu}_3\text{O}_{7-\delta}$ leads to the conclusion that the coupling constant λ associated with the excitation driving the linear resistivity is around 0.4.⁴ Clearly this provides a rather stringent upper bound on the electron-phonon coupling constant. Furthermore, the lifetime is found to be rather insensitive to carrier concentration in the metallic regime,^{4,5} so that the large decrease in the dc conduc-

tivity as the insulator is approached, must then be attributed to an increase in m^*/n . From these measurements it is not possible to distinguish whether the approach to the insulator is related to a large effective mass m^* , such as in a localization model of the insulator or to a small carrier number n , which might be more appropriate to a system with a gap [such as found in the Hubbard split band or spin-density wave (SDW) models] which persists into the metallic phase. Nevertheless, these measurements of m^*/n serve to emphasize the point that Coulomb correlation effects of one form or another are clearly manifested in the dc resistivity and must be included in any calculation of the electron-phonon coupling constant. Previous estimates of the electron-phonon coupling constant λ in $\text{La}_{2-x}\text{Sr}_x\text{CuO}_4$ range from 0.65 to 2.0.^{2,3} In $\text{YBa}_2\text{Cu}_3\text{O}_{7-\delta}$ the values lie between 0.32 and 2.9.^{2,6} For the most part these numbers are in excess of the upper bound imposed by the ac conductivity Drude fits.

Our approach to calculations of the electron-phonon interaction is based on a Fermi-liquid scheme which we have discussed elsewhere.⁷ We build on the heavy-fermion literature⁸ to treat the Anderson lattice or extended Hubbard Hamiltonian in the presence of infinite Coulomb correlations U on the Cu sites. Our starting Hamiltonian for the copper oxide plane in the auxiliary-boson formulation⁸ is given by

$$H_0 = \sum_{i,\sigma} \epsilon_d^0 d_{i,\sigma}^\dagger d_{i,\sigma} + \sum_{j,\sigma} \epsilon_p C_{j,\sigma}^\dagger C_{j,\sigma} + \sum_{i,j,\sigma} V(d_{i,\sigma}^\dagger \mathbf{e}_i C_{j,\sigma} + \text{H.c.}) + \sum_{j,l,\sigma} t(C_{j,\sigma}^\dagger C_{l,\sigma} + \text{H.c.}), \quad (1)$$

with a constraint equation at each site

$$\sum_{\sigma} d_{i,\sigma}^\dagger d_{i,\sigma} + \mathbf{e}_i^\dagger \mathbf{e}_i = 1, \quad (2)$$

where the creation operators C^\dagger and d^\dagger represent oxygen and copper electronic states, respectively. In this "electron" picture the mixed valence states consist of Cu^{2+} and Cu^{3+} . We could equally well work in the infinite- U "hole

picture" where the allowed states are Cu^{2+} and Cu^{1+} , although in this case we would need to assume somewhat smaller values⁹ of the hybridization in order to obtain the same physical picture. Applying a mean-field approximation to Eq. (1) leads to a renormalized band structure in which the copper-oxygen hybridization is substantially reduced and the d level raised toward the Fermi energy. At half filling the renormalized hybridization vanishes identically signaling the breakdown of the Fermi liquid due to localization ($m^* \rightarrow \infty$). Indeed, within a strict Fermi-liquid theory in which the Fermi volume contains the full complement of carriers, the carrier number n does not vanish but rather approaches unity at the insulating limit. An appreciably enhanced mass is therefore a necessary consequence of any (Luttinger sum rule obeying) Fermi-liquid picture, which is also compatible with the low-frequency conductivity data discussed above.

We deduce the electron-phonon coupling constants in two ways using this Hamiltonian. The first, a "frozen-phonon" (FP) scheme introduces the phonon as a static distortion of the lattice. The electronic eigenenergies are then recalculated in the presence of the distortion and their corresponding shifts can be used to deduce the electron-phonon coupling. Alternatively a diagrammatic screening approach¹⁰ has been used which is based on equivalent RPA treatments of the electron gas. Here the "Kondo boson" or $1/N$ fluctuation contribution⁸ plays the role of the usual screened Coulomb term, and N is the degeneracy of the Cu and oxygen spin states. In this paper we focus exclusively on the frozen-phonon approach, although the physics in both approaches is very similar. For definiteness, we assume a wave vector $\mathbf{Q} = \mathbf{X} = (\frac{1}{2}, \frac{1}{2}, 0)(\pi/a)$ for the FP distortion. The electron-phonon interaction is written as

$$H_{e\text{-ph}} = H_{\text{FP}} - H_0$$

$$= \sum_{\mathbf{k}, \sigma, \nu} g_{\mathbf{Q}, \nu} \left(\frac{\hbar}{2N_I M_\nu \omega_{\mathbf{Q}, \nu}} \right)^{1/2} \alpha_{\mathbf{k}+\mathbf{Q}}^\dagger \alpha_{\mathbf{k}} (a_{\mathbf{Q}, \nu}^\dagger + a_{-\mathbf{Q}, \nu}), \quad (3)$$

where α^\dagger denotes the creation operator for the quasiparticles near the Fermi surface, calculated for the undistorted Hamiltonian. The electron-phonon transition matrix element is

$$g_{\mathbf{Q}, \nu} = \lim_{\delta R \rightarrow 0} \left\langle a_{\mathbf{k}+\mathbf{Q}, \sigma} \left| \frac{\delta H}{\delta R} \cdot \hat{\varepsilon}_{\mathbf{Q}, \nu} \right| a_{\mathbf{k}, \sigma} \right\rangle. \quad (4)$$

For notational simplicity, we do not write down the distorted Hamiltonian; it can be readily deduced from Eq. (1) when ε_p and ε_d are assumed to be site dependent due to the bond-length dependence of V and t . In Eq. (4) the input parameters^{11,12} which set the scale for the strength of the electron-phonon coupling are, in the linear approximation, $V(R+\delta R) - V(R) \approx -7V\delta R/a$, and $t(R+\delta R) - t(R) \approx -2t\delta R/a$ where R denotes the copper-oxygen bond length. (Similar variations arising from ε_d and ε_p can be also be included.) The distortion of $\mathbf{Q} = \mathbf{X}$ introduces at most two inequivalent sites for these variables and the various site dependences are dictated by the sym-

metries of the static mode under consideration.

Here we consider only planar distortions such as would be appropriate to phonons in $\text{La}_{2-x}\text{Sr}_x\text{CuO}_4$, although the behavior of the resistivity in $\text{YBa}_2\text{Cu}_3\text{O}_{7-\delta}$, to which we will also refer, does not appear to be different by more than factors of 2 or 3.¹ The distortions which have been discussed elsewhere,¹³ are categorized according to their planar projections into six distinct types, shown in the inset of Fig. 1. We use known results to associate with each of these a corresponding phonon frequency $\omega_{\mathbf{Q}, \nu}$. Because the out-of-plane motion leads to a further subdivision of these six modes¹³ (into 15) we treat all 15 frequencies as distinct. The mean-field approximated Hamiltonians are readily written in a 6×6 matrix form. Within this matrix formalism, the band structure is numerically determined in the presence of the variational conditions on the two inequivalent boson amplitudes e_0 and Lagrange multipliers. Physically these variational or self-consistent conditions impose strong "screening" constraints on the electron-phonon coupling. This screening is a consequence of infinite Coulomb correlations on the copper site which make it difficult to transfer charge when these sites are close to half full. This effect is rather dramatic and is illustrated in Fig. 1 which plots the six electron-phonon transition matrix elements as a function of the dopant concentration. Near the half filling limit all the coupling constants vanish as $e_0^2 \propto (1 - n_d)$. It should be noted that somewhat before the insulating state is reached the entire frozen phonon picture will break down, since then the electronic energy scales become comparable¹⁰ to those of the phonons and the static or frozen-phonon approximation is not valid.

The effects of this reduced electron-phonon coupling, as well as the enhanced effective masses have important implications for the transport properties of the copper oxides. We calculate the resistivity¹⁴ from the linearized

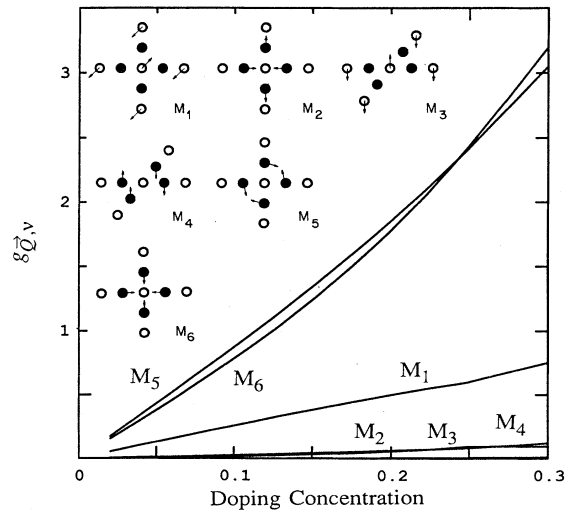


FIG. 1. Concentration dependence of the electron-phonon coupling constant for the six planar modes discussed in the text. The open and solid circles indicate copper and oxygen, respectively.

Boltzmann transport equation as

$$\rho = \frac{V_0}{e^2} \frac{1}{\langle\langle v_{k_x}^2 \rangle\rangle_{\text{FS}} N(E_F)} \frac{1}{\tau}, \quad (5)$$

where the electron-phonon scattering rate is given by

$$\frac{1}{\tau_{e\text{-ph}}} = \frac{4\pi k_B T}{\hbar} \int_0^\infty d\omega \alpha_{\text{tr}}^2 F(\omega) \frac{I(\omega/2k_B T)}{\omega}, \quad (6)$$

and $I(y) = (y/\sinh y)^2$. Here we approximate the phonon transport spectral function by

$$\alpha_{\text{tr}}^2 F(\omega) = \frac{\langle\langle [v_{k_x} - v_{k_x'}]^2 |g_{\mathbf{Q},\nu}|^2 \rangle\rangle_{\text{FS}}}{4\langle\langle v_{k_x}^2 \rangle\rangle_{\text{FS}}} \times \frac{\hbar}{N_1 M_\nu \omega_{\mathbf{Q},\nu}} N(E_F) \delta(\omega - \omega_{\mathbf{Q},\nu}), \quad (7)$$

and we have assumed that the more complicated \mathbf{k} -space summations can be replaced by Fermi surface averaging¹⁵ $\langle\langle \rangle\rangle_{\text{FS}}$. The quantity (n/m^*) which appears in the simple formula for the resistivity $\rho = (m^*/ne^2)(1/\tau)$ can be readily calculated from the (undistorted) band structure in terms of the Fermi surface averaged velocities and densities of states $N(E_F)$ using Eq. (5). In Fig. 2 we plot the inverse of this quantity as a function of hole concentration. We also indicate in the figure the corresponding value for the Drude plasma frequency $4\pi ne^2/m^*$. Experimental values for this plasma frequency range from 0.4 to 1.0 eV in $\text{La}_{2-x}\text{Sr}_x\text{CuO}_4$ (Refs. 1 and 16) and from 0.8 to 3.0 eV in $\text{YBa}_2\text{Cu}_3\text{O}_{7-\delta}$.^{17,18} The average value for both in the literature is around 1 eV which is about a factor of 10 less than a typical metal such as copper.¹⁹ The concentration dependence of our results is roughly seen experimentally.^{4,5}

The inset plots the electron-phonon lifetime which we calculate at 100 K. Despite strong screening effects this scattering is still about 10 times stronger than in copper.¹⁹

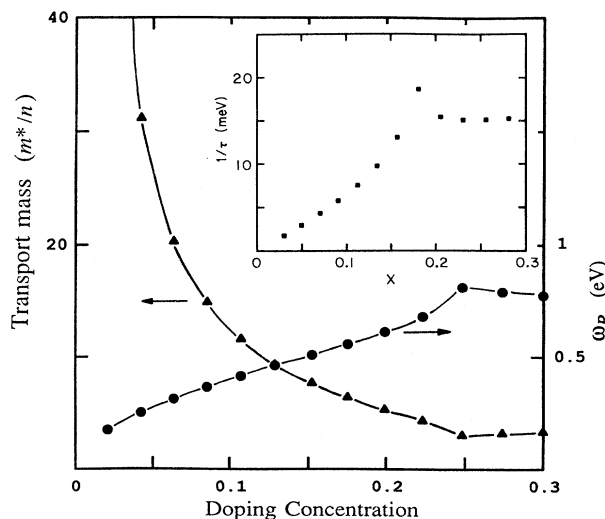


FIG. 2. Concentration x dependence of transport mass (or plasma frequency). The inset plots the electron phonon lifetime vs x at 100 K. The small kinks reflect van Hove singularities.

This together with the ten times smaller Drude plasma frequency can help explain why the resistivity slopes are roughly 2 orders of magnitude larger than in copper. It should be noted that the corresponding value for the coupling constant λ which we find is considerably less than most *theoretical* values in the literature. By contrast, experimental measurements of the dc scattering rate at 100 K range^{4,5} between about 15 and 30 meV which are rather close to our estimates based only on the electron-phonon contribution.

By combining the lifetime with (n/m^*) , we can calculate the temperature and concentration-dependent resistivity. The temperature dependence of ρ is shown in the inset of Fig. 3 for $x = 0.20$ in arbitrary units. This curve is close to but clearly not precisely linear. In order to quantitatively compare the electron-phonon contribution with the measured values, we represent the resistivity by its slope $d\rho/dT$, so as to avoid uncertainties in the residual resistivity. Shown in Fig. 3 are a collection of experimental data^{5,20,21} on $\text{La}_{2-x}\text{Sr}_x\text{CuO}_4$ (squares, triangles, and circles). The solid line plots our theoretical results at $T = 300$ K. It can be seen in the theory that the concentration dependence of the slope is rather weak, since the increase in the effective mass tends to cancel out the decrease in the electron-phonon scattering as the insulator is approached. Experimentally, the slope shows an increase below about 10 or 15% hole concentration. Even in materials which are close to or actually insulating, there appears to be a linear contribution at high temperatures with even higher slope, as indicated by the few data points in this regime.^{5,21} It is interesting to try to analyze these data by adding to our calculated electron-phonon scattering an additional concentration-independent transition matrix element leading to a small additional relaxation time $1/\tau_0 \approx 3.5$ meV well into the metallic regime. The

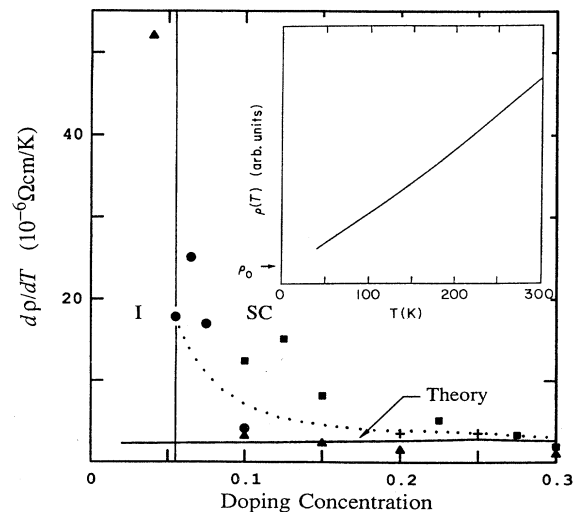


FIG. 3. Concentration dependence of the resistivity slope at 300 K. Theoretical results dotted (or solid lines) are with (or without) a small phenomenological added constant lifetime. Triangles, circles, squares (and crosses) are from Refs. 5, 21, and 20, respectively. The inset plots the calculated temperature-dependent resistivity at $x = 0.20$.

net effect yields a rather concentration-independent τ throughout the entire superconducting region, as seems consistent with the data.^{4,5} This results in a small correction to $d\rho/dT$ for $x > 0.17$, but as the insulator is approached, the slope shows a rapid rise, mirroring the behavior of the transport mass. The results of this phenomenological analysis are shown by the dotted curve, which seems to semiquantitatively reproduce the trends in the data. In some sense this additional scattering time can be viewed as representing the size of the "error" made by ignoring all other scattering mechanisms but the two-dimensional copper-oxide phonons. Other phonons or, perhaps, magnetic scattering effects may account for the size of this term.

The striking observation that saturation does not occur in the copper oxides has been used by Gurvitch and Fiory¹ to deduce an upper bound on the electron-phonon coupling constant. In both $\text{YBa}_2\text{Cu}_3\text{O}_{7-\delta}$ and $\text{La}_{2-x}\text{Sr}_x\text{CuO}_4$, the maximum λ is of order of a few tenths, with a plasma frequency $\omega_p \approx 1$ eV. These upper limits are reasonably consistent with the τ and n/m^* values deduced from Drude fits which suggests that these materials have mean free paths which are close to but not less than the minimum value of a few copper-oxide lattice spacings. Our own, more microscopically based estimates lead to the same conclusion. As an input to this calculation we find an effective Fermi velocity of about 0.4×10^7 cm/sec to 0.8×10^7 cm/sec. Interestingly enough, if we use the phenomenologically adjusted relaxation time shown by the dotted line in Fig. 3, we find that at around 5–7% hole concentration the mean free path coincides with the bond length. Thus the Mott-Ioffe-Regel criterion¹ for metallic conductivity is violated about where the materials are found to go insulating.

In conclusion, in the present picture the copper oxides

are viewed as moderately heavy Fermi liquids. The enhancement of the transport mass which is of order 10 in the metallic regime becomes progressively larger (varying as the inverse of the carrier concentration) as these systems approach the insulating limit. Electron-phonon contributions to the resistivity lead to resistivity slopes which are within a factor of 2 of experiment. While we cannot argue that this is the entire source of the temperature-dependent resistivity, it is likely that this is the dominant effect. It should be stressed that the calculated m^*/n and lifetime components to the low-frequency conductivity ($\omega_p \approx 0.8$ eV and $1/\tau_{e-ph} \approx 15$ meV at 100 K, both of which are compatible with Drude measurements) are not directly related since the former derives from Coulombic and the latter from phononic contributions. These materials appear to be near the Mott-Ioffe-Regel criterion for the minimum mean free path which criterion seems to break down at about the critical concentration for the metal-insulator transition. Our calculations lead to a suppression of the electron-phonon interaction as the insulator is approached. This strong screening of the electron-phonon interaction makes it unlikely that phonons are related in any important way to the superconductivity and may also bear on other charge fluctuation models for the superconducting transition.

This work was submitted in partial fulfillment of the Ph.D. requirement at the University of Chicago. Useful conversations with G. Thomas, T. F. Rosenbaum, and S. Nagel are acknowledged. This work was supported by the National Science Foundation Grant No. STC-8809854, Materials Research Laboratory Grant No. DMR-16892, and U.S. Department of Energy Grant No. DE-AC02-76H00016. A.A. acknowledges partial support from the Sloan Foundation.

*Present address: Physics Department 510A, Brookhaven National Laboratory, Upton, NY 11973, and Physics Department SUNY, Stony Brook, NY 11794.

¹M. Gurvitch and A. T. Fiory, Phys. Rev. Lett. **59**, 1337 (1987).

²P. B. Allen, W. E. Pickett, and H. Krakauer, Phys. Rev. B **37**, 7482 (1988).

³W. Weber, Phys. Rev. Lett. **58**, 1371 (1987).

⁴G. A. Thomas (private communication); J. Orenstein, G. A. Thomas, A. J. Millis, S. L. Cooper, D. H. Rapkine, T. Timusk, L. F. Schneemeyer, and J. V. Waszczak (unpublished).

⁵M. Suzuki, Phys. Rev. B **39**, 2312 (1989); M. Suzuki (unpublished).

⁶R. Zeyher and G. Zwirner, Solid State Commun. **66**, 617 (1988).

⁷J. H. Kim, K. Levin, and A. Auerbach, Phys. Rev. B **39**, 11633 (1989).

⁸A. Auerbach and K. Levin, Phys. Rev. Lett. **57**, 877 (1986); A. J. Millis and P. A. Lee, Phys. Rev. B **35**, 3394 (1987).

⁹G. Kotliar, P. A. Lee, and N. Read, Physica C **153–155**, 538 (1988).

¹⁰J. H. Kim, K. Levin, R. Wentzcovitch, and A. Auerbach (unpublished).

¹¹W. A. Harrison and S. Froyen, Phys. Rev. B **21**, 3214 (1980).

¹²A. K. McMahan, R. M. Martin, and S. Satpathy, Phys. Rev. B **38**, 6650 (1988).

¹³R. E. Cohen, W. E. Pickett, H. Krakauer, and L. L. Boyer, Physica B **150**, 61 (1988).

¹⁴P. B. Allen, Phys. Rev. B **17**, 3725 (1978).

¹⁵J. L. Martins and M. L. Cohen, Phys. Rev. B **37**, 3304 (1988).

¹⁶S. Tajima, S. Uchida, H. Ishii, H. Takagi, S. Tanaka, U. Kawabe, H. Hasagawa, T. Aita, and T. Ishiba, Mod. Phys. Lett. B **1**, 353 (1988).

¹⁷D. A. Bonn, A. H. O'Reilly, J. E. Greedan, C. V. Stager, T. Timusk, K. Karama's, and D. B. Tanner, Phys. Rev. B **37**, 1574 (1988).

¹⁸Z. Schlesinger, R. T. Collins, D. L. Kaiser, and F. Holtzberg, Phys. Rev. Lett. **59**, 1958 (1987).

¹⁹See, for example, D. Pines, *Elementary Excitations in Solids* (Benjamin/Cummings, Reading, 1963); N. W. Ashcroft and N. D. Mermin, *Solid State Physics* (Saunders College, Philadelphia, 1976).

²⁰J. M. Tarascon, L. H. Greene, W. R. McKinnon, G. W. Hull, and T. H. Geballe, Science **235**, 1373 (1987); C. Uher, A. B. Kaiser, E. Gmelin, and L. Walz, Phys. Rev. B **36**, 5676 (1987).

²¹B. Ellman, H. M. Jaeger, D. P. Katz, T. F. Rosenbaum, A. S. Cooper, and G. P. Espinosa, Phys. Rev. B **39**, 9012 (1989).